PNAS RESEARCH ARTICLE | ECOLOGY

Ancient DNA suggests a historical demographic decline and genetic erosion in the Atlantic bluefin tuna

Adam Jon Andrews[a,b,1], Emma Falkeid Eriksen[c], Bastiaan Star[c], Kim Præbel[d], Antonio Di Natale[e], Estrella Malca[f,g], Vedat Onar[h], Veronica Aniceti[i], Gabriele Carenti[j], Gäel Piquès[k], Svein Vatsvåg Nielsen[l], Per Persson[m], Federica Piattoni[b], Francesco Fontani[n], Lane M. Atmore[c,o], Oliver Kersten[c], Fausto Tinti[b,1], Elisabetta Cilli[n,2], and Alessia Cariani[b,2]

Affiliations are included on p. 9.

Edited by Barbara Block, Stanford University, Pacific Grove; received May 13, 2024; accepted April 8, 2025

Overexploitation has depleted fish stocks during the past century; nonetheless, its genomic consequences remain poorly understood for most species. Characterizing the spatiotemporal patterns of these consequences may provide baseline estimates of past diversity and productivity to aid management targets, help predict future dynamics, and facilitate the identification of evolutionary factors limiting fish population recovery. Here, we evaluate human impacts on the evolution of the iconic Atlantic bluefin tuna (*Thunnus thynnus*), one of the longest and most intensely exploited marine fishes, with a tremendous cultural and economic importance. We sequenced whole genomes from modern (n = 49) and ancient (n = 41) specimens dating up to 5,000 y ago, uncovering several findings. First, we identify temporally stable patterns of population admixture, as bluefin tuna caught off Norway and in the eastern Mediterranean share a greater degree of ancestry with Gulf of Mexico bluefin tuna than western and central Mediterranean bluefin tuna. This suggests that Atlantic spawning areas are important mixing grounds for the genetic diversity of Mediterranean bluefin tuna. We model effective population size to show that Mediterranean bluefin tuna began to undergo a demographic decline by the year 1900 to an extent not observed across the previous millennia. Coinciding with this, we found that heterozygosity and nucleotide diversity were significantly lower in modern (2013 to 2020) than ancient (pre-1941) Mediterranean bluefin tuna, suggesting that bluefin tuna underwent a genetic bottleneck. With this work, we show how ancient DNA provides unique perspectives on ecological complexity with the potential to inform the management and conservation of fishes.

conservation genomics | ancient DNA | historical ecology | population genetic bottleneck | overfishing

Significance

Achieving the aim of the current UN Ocean Decade to "protect and restore ecosystems and biodiversity" is stymied by a lack of historical knowledge on how human exploitation has impacted and therefore what should be restored. Here, we sequence DNA in ancient fish bones to evaluate the historical diversity of the Atlantic bluefin tuna, which has been of great commercial importance for centuries. We find that bluefin tuna began to undergo demographic decline by 1900, 70 y earlier than currently recognized. Correspondingly, we find that modern bluefin tuna had lower levels of genetic diversity than historical ones. This suggests that human impacts on the diversity of marine fishes are likely to have begun earlier and be more complex than previously thought.

As we restore our oceans, fundamental questions remain as to how productive fish populations were historically and whether their recovery and adaptability will be hampered by genetic changes like a loss of genetic diversity, which could have resulted from their exploitation (1, 2). Between 1970 and 2007, the ecologically, culturally, and commercially important pelagic fish, Atlantic bluefin tuna (*Thunnus thynnus; hereafter bluefin tuna*), was severely depleted, resulting in the loss of large size classes and rarity across its range, where it periodically disappeared from habitats such as the North, Norwegian, and Black Seas (3–8). Fisheries data from recent decades estimate that between 1960 and 2009, the eastern stock abundance and range declined by an estimated 70% and 46 to 53%, respectively (4, 5). Mediterranean bluefin tuna stock abundance has recently recovered to 1970s levels following several years of international management and favorable oceanographic conditions, while it has returned to most of its previous habitats (9–13).

Bluefin tuna recovery is duly considered a fisheries management success (3, 14); as a result, catch quotas have increased since 2018 (13). However, historical sources suggest that the intensification of bluefin fisheries—and subsequent population declines—had begun centuries previously (15), indeed bluefin tuna have been commercially fished in the Mediterranean since before ancient Greek times. This trend has been shown for other marine populations and taxa [e.g., (16–19)], yet, little is known whether 1970 abundance baselines underestimate historical bluefin tuna productivity, and how centuries of exploitation have impacted its population structure, gene flow, and genetic diversity. This information could be useful to predict future population dynamics, protect sustainability, and maximize fisheries productivity (20–23). With this work, we use ancient DNA and whole genome sequencing to address these questions.

Bluefin tuna is characterized by its large size (up to 3.3 m in length and 725 kg in weight), far-reaching and inshore migration behavior, and slow maturation [between 3 and 12 y,

Author contributions: A.J.A., F.T., E.C., and A.C. designed research; A.J.A., E.F.E., B.S., K.P., E.M., V.O., V.A., G.C., G.P., S.V.N., P.P., F.P., F.F., L.M.A., O.K., F.T., E.C., and A.C. performed research; A.J.A., E.F.E., K.P., F.P., F.F., L.M.A., and O.K. analyzed data; and A.J.A., E.F.E., B.S., A.D.N., and F.T. wrote the paper.

The authors declare no competing interest.

This article is a PNAS Direct Submission.

[1]To whom correspondence may be addressed. Email: adam@palaeome.org or fausto.tinti@unibo.it.

[2]E.C. and A.C. contributed equally to this work.

This article contains supporting information online at https://www.pnas.org/lookup/suppl/doi:10.1073/pnas.2409302122/-/DCSupplemental.

Published May 20, 2025.

(24, 25)]. Recent genomic studies (26, 27) support the delineation of two highly connected populations, which are managed as two stocks (Fig. 1). These are a western Atlantic component that spawns predominantly in the Gulf of Mexico (28) and an eastern Atlantic and Mediterranean component that spawns predominantly in several high-productivity areas of the Mediterranean Sea (25). Mature and juvenile individuals of both populations migrate into the Atlantic Ocean to feed (29, 30), and exhibit high levels of mixing (26, 27). The role of other understudied and potential spawning areas such as those in the Azores, Canary Islands, and the Bay of Biscay (25, 31) is yet to be clearly defined, but bluefin tuna born in the Slope Sea [East of Cape Hatteras, USA, (28, 32)] appear to be a genetically mixed component of the two populations (27, 33). Due to the recent mismatch in recovery between the stocks and uncertainties on the scale of the decline in the western population(s) in the 1960s (3), there is concern about the genetic homogenization of the populations (33). In addition, there are many unknowns regarding migration and population structure, and while tagging and historical fishery data suggest that a portion of Mediterranean bluefin tuna is resident year-round (6, 34–36), there is as yet no genetic evidence for this.

For millennia, tuna traps have lined eastern Atlantic and Mediterranean coasts, intercepting spawning migrations of highly revered bluefin tuna between April and September (15, 29). By the 1600 to 1800s, Mediterranean bluefin tuna seemingly shifted habitat and diet preferences further from shore (37) and catches fluctuated heavily (38) indicating that the population was dynamic and varied potentially due to climate or early anthropogenic impacts. From 1800 to 1900, large bluefin tuna were increasingly targeted in trap fisheries, indicating the potential for fisheries-induced evolution (39). Trap records suggest that by the 1880s, landings had reached comparable levels to the 1980s to 2000s, the most intensive decades in bluefin tuna exploitation (3, 40). By 1970, the bluefin tuna range contraction away from the North, Norwegian, and Black Seas and the closure of the majority of the trap fisheries—suggests that the fishery's productivity was depressed (6). Therefore, we hypothesized that longer-term data are required to investigate demographic changes, and its impact, prior to the 1970s, from when routine fisheries data exist.

Genomic analyses of temporal samples before and after overexploitation events provide key opportunities to test for the onset of overexploitation and its impact on population structure and genetic diversity (22, 41, 42). In studies on fishes, recent demographic history has been modeled using modern samples to reveal preindustrial exploitation impacts in Atlantic herring (*Clupea harengus*) (16), but analyses directly testing genetic changes between temporal samples—e.g., to reveal signatures of genetic erosion—remain rare. This approach has been demonstrated in taxa, like seabirds and marine mammals (23, 42–44). Genetic erosion (the loss of genetic diversity e.g. heterozygosity, nucleotide diversity) may leave populations with lowered adaptive capacity and remains poorly studied in marine fishes due to technical limitations, including poor access to ancient genomes and genome-wide markers (45–49).

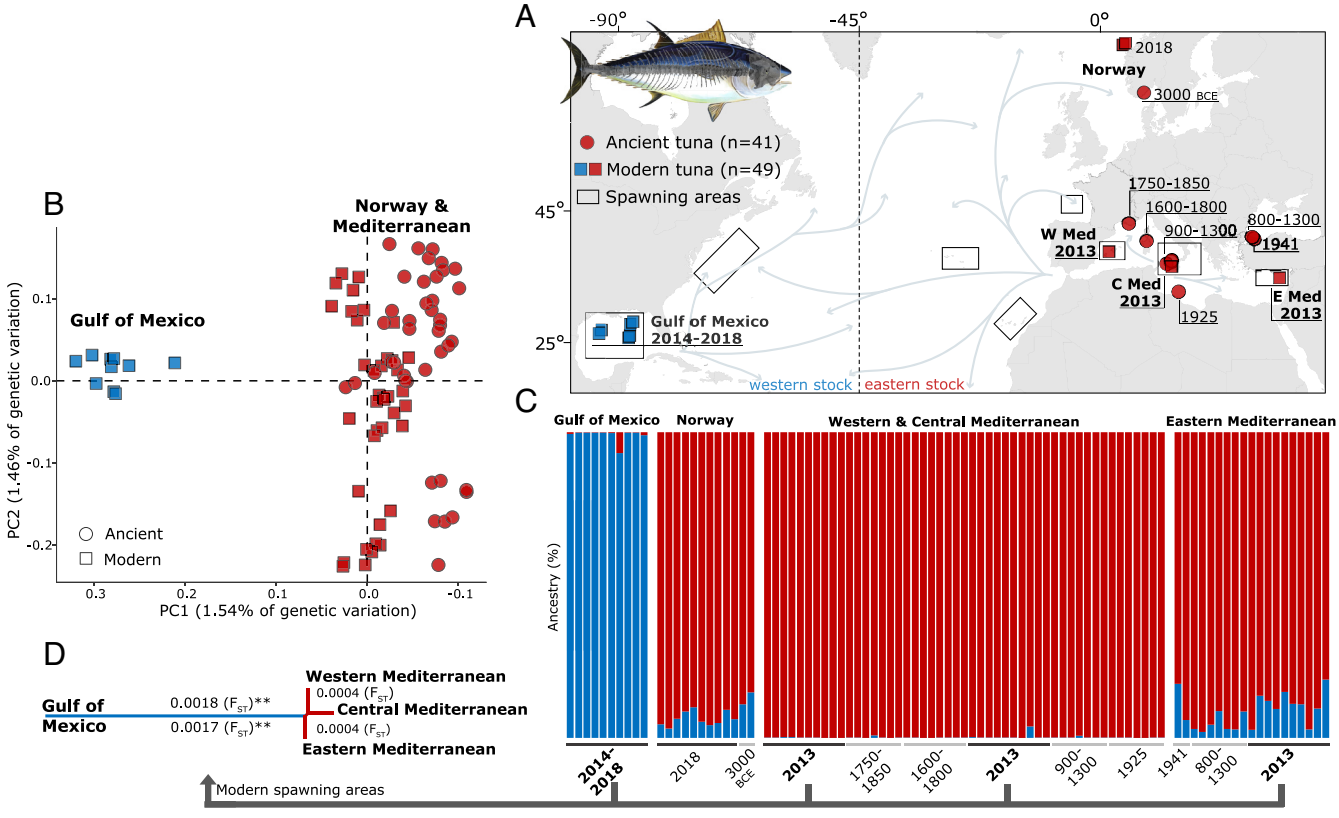

Fig. 1. Spatial patterns in admixture of the two Atlantic bluefin tuna (*Thunnus thynnus*) populations consistent over millennia, and map (*A*) of samples sequenced, spanning over millennia across the species range. Samples (named by year) are colored by stock: western stock (blue) and eastern stock (red). Ancient samples analyzed (n = 41) are depicted using circles, modern (n = 49) using squares. Modern larvae or YoY (young-of-the-year) samples from spawning sites are Gulf of Mexico, Western (W Med), Central (C Med), and Eastern (E Med) Mediterranean. Spawning areas are approximately depicted using rectangles, including Atlantic sites not sampled. Norwegian samples do not represent a spawning site. Gray arrows indicate stock distribution, mixing, and migration routes. Stock management line at 45°W is illustrated as a dashed black line. Map created using ESRI ArcMap (v.10.6, https://arcgis.com). Principal components analysis (PCA, *B*) using 12,838 SNPs shows two main sample clusters representing the western and eastern stocks. STRUCTURE barplot (*C*) using the same dataset shows ancestry proportions for the optimal number of populations (K = 2), tested using the Evanno Method, and evidence for increased Western Atlantic admixture in Norwegian and Eastern Mediterranean individuals, consistent across millennia. Pairwise F_{ST} neighbor joining tree (*D*) shows differentiation between modern spawning area samples at 386,963 loci, supporting STRUCTURE results. Statistical significance was indicated using FDR-corrected *P*-values (***P* <0.001).

Here, we publish whole-genome data on Atlantic bluefin tuna including a long time series of genome-wide aDNA data, analyzing 41 archaeological and archived bones from seven Mediterranean and Norwegian locations, dated from ca. 3000 BCE to 1941 CE (Fig. 1). Using whole-genome sequencing data of a further 49 modern individuals caught in the Mediterranean, Norway, and the Gulf of Mexico between 2013 and 2018, we investigate population admixture, effective population size, and genetic diversity over time to test for the impact of overexploitation on bluefin tuna demography.

Results

We analyzed over 19.8 billion sequencing reads, obtaining an average of 9.9-fold nuclear coverage for the ancient and 11.9-fold coverage for the modern samples (Table 1 and *SI Appendix*, Table S1). Ancient samples showed excellent preservation with relatively high proportions of endogenous DNA (average 40.4%), while containing fragmentation and sequence damage patterns (increases in C > T and G > A transitions) that are expected from authentic, degraded DNA (Table 1 and *SI Appendix*, Fig. S1). We mapped all reads to a pseudochromosome reference genome produced from high-quality, short-read data for the species and—following an extensive set of quality-filtering steps (*Methods and Materials*)—we analyzed single-nucleotide polymorphisms (SNPs) in 90 individuals using approaches based on hard called genotypes. Overall, these filters produced final pruned datasets of 386,963 loci for modern spawning area samples and 12,838 loci when combining modern and ancient samples. This represented a ca. 15-fold increase in genomic representation compared to previous attempts investigating modern bluefin tuna demography (33), and over a 100-fold increase when using ancient DNA (46, 50).

Patterns of Population Mixing Consistent Across Millennia. We found that the most likely number of bluefin tuna populations (K) described by PCA and STRUCTURE was two, represented by one genomic cluster for the Gulf of Mexico, and one for Norway and the Mediterranean (Fig. 1 *B*–*D* and *SI Appendix*, Fig. S2). We found increased (ca. 10%) western-Atlantic ancestry in individuals caught off Norway and in the Eastern Mediterranean—which was consistent in ancient samples dating back up to 3000 BCE from the same areas (Fig. 1*C*), and at 386,963 loci for the modern spawning site dataset (*SI Appendix*, Fig. S3). Bluefin tuna from Western and Central Mediterranean sites, over a millennium, shared similar ancestry proportions to each other, with lower Gulf of Mexico-like ancestry and increased Mediterranean ancestry than Eastern Mediterranean individuals (Fig. 1*C*).

Pairwise F_{ST} values (Fig. 1*D*) across 386,963 loci for modern spawning sites support admixture patterns where Eastern Mediterranean individuals are slightly more closely related to Gulf of Mexico individuals than the Western and Central Mediterranean are (0.0017 vs 0.0018 F_{ST}). Overall, differences between the Western and Eastern Atlantic are low but significant ($P = 0.007$). Patterns of population structure appear unbiased by our loci filtering choices on both modern and ancient datasets (*SI Appendix*,

Table 1. Summary details of ancient and modern Atlantic bluefin tuna samples sequenced herein

Year	Location/ archaeological site	Latitude	Longitude	Sample type	n sampled	Sequence Length (mean bp)	Endogenous (mean%)	n in final analysis	Sequencing Coverage (mean X)
2018	Møre, Norway	61.99	4.34	Adult	10	100 ± 1	83 ± 1	10	13.2 ± 3.6
2014-2018	Gulf of Mexico	26.0*	−90.0*	Larvae	10	79 ± 17	61 ± 0	10	10.0 ± 2.1
2013	Western Mediterranean	39.27	2.10	Young of the Year	10	80 ± 21	68 ± 0	10	11.4 ± 3.6
2013	Central Mediterranean	36.93	13.17	Young of the Year	10	81 ± 19	56 ± 0	10	12.2 ± 3.6
2013	Eastern Mediterranean	35.51	33.41	Young of the Year	10	116 ± 19	71 ± 0	9	13.4 ± 2.7
1941	Istanbul, Türkiye	41.00	28.95	Archived adult bone	2	66 ± 4	19 ± 11	2	9.7 ± 4.7
1925	Zliten, Libya	41.00	14.65	Archived adult bone	8	70 ± 10	41 ± 5	8	10.3 ± 4.0
1750-1850	Marseille, France	43.30	5.36	Archaeological adult bone	7	68 ± 8	26 ± 5	7	9.5 ± 2.9
1600-1800	Sassari, Italy	40.86	8.62	Archaeological adult bone	9	72 ± 7	50 ± 7	8	8.3 ± 0.9
900-1300	Sicily, Italy	37.65*	12.58*	Archaeological adult bone	7	71 ± 8	39 ± 13	6	10.3 ± 1.9
800-1300	Istanbul, Türkiye	41.00	28.95	Archaeological adult bone	10	74 ± 6	54 ± 5	8	9.1 ± 5.2
3000 BCE	Jortveit, Norway	58.27	8.51	Archaeological adult bone	2	70.5 ± 10	64 ± 5	2	20.5 ± 10.5

n = number. Gulf of Mexico and Sicily samples pertain to several sites; for full details, see *SI Appendix*, Table S1.

Figs. S3 and S4). Our results were not driven by recently discovered introgression, which was identified on Chromosome 8 and was filtered out (along with other deviations from HWE, see *Methods and Materials* and *SI Appendix*, Figs. S5 and S6) on the basis that they are not population-defining characteristics (33).

A Historical Demographic Decline and Genetic Erosion. Reconstructions of historical effective population size (N_e) using GONE reveal significant N_e decreases in both the Gulf of Mexico and Mediterranean spawning area samples between 1850 and 1900 (Mediterranean: $P < 0.001$, $R^2 = 0.15$, $F = 27.7_{149}$ linear regression), corresponding to a period of intensive exploitation. Runs of homozygosity (RoH) show inbreeding extent (fraction of genome in RoH, FRoH) varied slightly between modern spawning areas where there are no significant differences in inbreeding between modern sample site groups (Fig. 2*B*, $P > 0.05$, Wilcoxon rank-sum).

Modern samples (2013 to 2018) had significantly lower nucleotide diversity and higher homozygosity (lower heterozygosity) than ancient samples (3000 BCE - 1941 CE, $P < 0.001$, Wilcoxon rank-sum, Fig. 2 *D* and *E*). Nucleotide diversity and homozygosity results show these are genome-wide patterns i.e. tens of thousands of loci spread across the genome but are subject to missing data at 2,890,241 loci (*SI Appendix*, Figs. S7 and S8). The loss of heterozygosity appears to have begun from the period of 1600 to 1800 (years) and declined step-wise, again after 1941 (*SI Appendix*, Fig. S9). Low sample size per group and spatial variance across the Mediterranean complicate inferences of a temporal trajectory but the same general stepwise trajectory of loss in nucleotide diversity is observed (*SI Appendix*, Fig. S10).

Population-specific F_{ST} was analyzed as a measure of expected heterozygosity which is theoretically less impacted by mutation and inbreeding than RoH (51, 52), where the most heterozygous sample is theoretically most ancestral (53). Population-specific F_{ST}s are lowest (most heterozygous i.e. ancestral) for the Gulf of Mexico, which shares overlapping CI with the Eastern Mediterranean, while the Central and Western Mediterranean (sharing overlapping CIs) have higher F_{ST}s (*SI Appendix*, Fig. S11), corroborating STRUCTURE and FRoH results. The Gulf of Mexico sample overlaps more with the Mediterranean samples in inbreeding extent (FRoH) than population-specific F_{ST} (Fig. 2 *C* and *D*). Lengths of RoHs were relatively short (<175 Kb) and did not vary between modern spawning sites (*SI Appendix*, Figs. S12 and S13).

The Gulf of Mexico sample and Mediterranean samples share similar N_e over millennia, beginning (from year 1000) with a period of long stability across centuries, before a significant decline around year 1850 to 1900, regardless of whether the Mediterranean samples are pooled (Fig. 2*A* and *SI Appendix*, Fig. S14). Significantly higher homozygosity for modern samples was consistent when removing transition sites which had the potential to be affected by postmortem

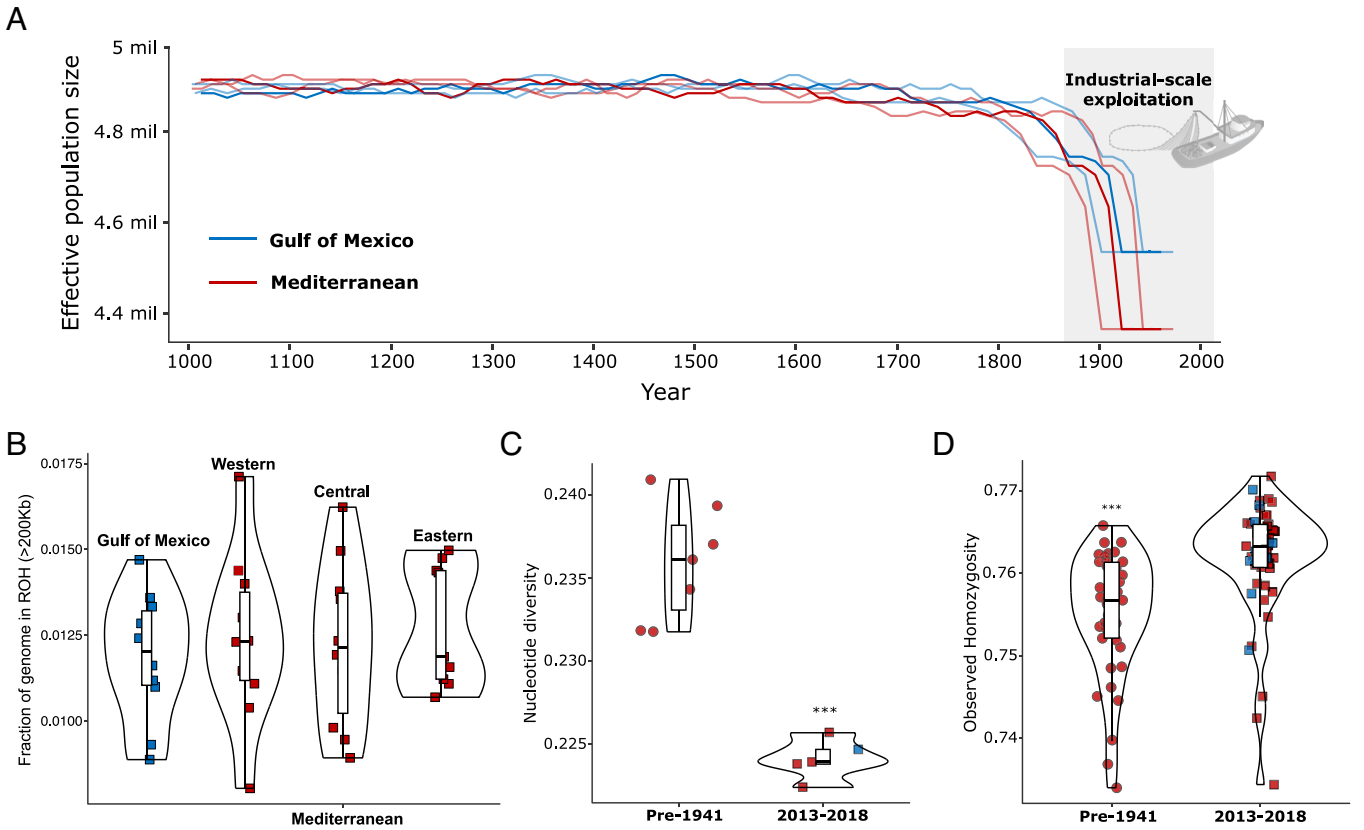

Fig. 2. Temporal demographic decline and genetic diversity loss in modern Atlantic bluefin tuna (*Thunnus thynnus*). (*A*) GONE reconstructions of historical effective population size (Ne) for the Gulf of Mexico (blue, n = 10) and Mediterranean (red, n = 29) populations using modern spawning site samples at 664,522 SNPs. Years for GONE estimates were calculated from generation numbers using three different generation lengths (10 to 16 y), showing the most likely (13 y) in full color, and 10 and 16 y slightly transparent. GONE plots do not include data more recent than 1973 due to the removal of estimates for the four most recent generations (*Methods and Materials*). Estimates were illustrated in relation to a potential causative exploitation event. (*B*) Violin plots show the fraction of the genome in runs of homozygosity (RoH) for each modern spawning area sample, at 664,522 unpruned SNPs. (*C*) Violin plots show nucleotide diversity (per sample group) differences at 2,890,241 SNPs including 10% missing data between pooled ancient (Pre-1941, sample groups = 7) and modern (2013 to 2018, sample groups = 5). (*D*) Violin plots show observed homozygosity (fraction of sites) differences at 17,741 SNPs between pooled ancient (Pre-1941, n = 41) and modern (2013 to 2018, n = 49). Significance of Wilcoxon rank-sum tests between the groups was illustrated for significant pairs using asterisk (***$P < 0.001$), boxplots illustrated with group medians, 25th and 75th percentile as outer edges, and 95th percentiles (black whiskers). Samples are colored by population (blue: western stock, red: eastern stock) where shapes depict time period (circle: ancient, square: modern).

DNA damage or when filtering for high-quality SNPs represented by at least 10 reads and GQ scores >25 (*SI Appendix*, Fig. S15 $P < 0.001$, Wilcoxon rank-sum). Modern samples also had higher overall homozygosity than ancient samples if we did not filter loci by F_{ST} and if we allow missing data (*SI Appendix*, Fig. S8 $P < 0.001$, Wilcoxon rank-sum). Finally, we found that with two different filtering techniques, homozygosity was not higher for low-coverage samples (*SI Appendix*, Fig. S16). F_{ST} differences between ancient and modern samples show that temporally variable loci are relatively low F_{ST} (<0.1) and do not display patterns across the genome indicative of selective sweeps (*SI Appendix*, Fig. S7).

Discussion

Here, we used ancient and modern whole-genome data of Atlantic bluefin tuna to assess genomic consequences of their exploitation, such as changes in population structure, admixture, and genetic diversity. We find evidence for two populations: a western and eastern Atlantic component that share high levels of connectivity, especially in bluefin tuna caught off Norway and the eastern Mediterranean. We find genomic evidence that bluefin tuna population(s) suffered a demographic decline by 1850 to 1900, and we correlate this observation with a loss in heterozygosity over the same period. Here, we contextualize our results with ecological, evolutionary, and historical perspectives.

Patterns of Population Mixing Consistent Across Millennia. Our study suggests bluefin tuna population structure has persisted across millennia, comprising two populations with low levels of differentiation. This finding is consistent with the ecology of bluefin tuna as a highly fecund batch spawner exhibiting wide-ranging migrations, high levels of population mixing, and large census sizes, as well with previously published genetic results (24–26, 33, 54). Low genetic divergence in bluefin tuna complicates the assessment of population structure. Nevertheless, we find small (ca. 10%), increased western Atlantic-like ancestry in Norwegian and Eastern Mediterranean samples that are consistent across millennia suggesting that these are true biological patterns.

These admixture patterns may be ecologically explained if bluefin tuna caught off Norway and in the eastern Mediterranean mix with Western Atlantic bluefin tuna. This phenomenon is likely in poorly understood Atlantic spawning areas, like the Slope Sea and Bay of Biscay or potential ones like the Azores and Canary Islands [Fig. 1; (25, 28, 31)]. Larvae with increased levels of admixture have indeed been found in the Slope Sea (33). Our results suggest this phenomenon varies between western and eastern Mediterranean bluefin tuna. While we cannot exclude the possibility that our results are due to error or small sample size, we find it unlikely that either can explain the temporal continuity in admixture through samples of various origins. We suggest that variation in bluefin tuna admixture within the Mediterranean was probably not found in the majority of previous studies due to the pooling of Mediterranean samples (33), or using small SNP datasets rather than whole genome sequencing done herein (26, 27). However, indications of genetic heterogeneity within Mediterranean bluefin tuna have indeed been made previously e.g. (55, 56) that corroborate our findings. Furthermore, greater genetic connectivity between the Atlantic and Eastern—rather than Western—Mediterranean spawning grounds is a component of other marine fishes (57–59), potentially driven by a spawning behavior established when Atlantic species recolonized the Mediterranean at the end of the last glacial maximum (60).

Theories of resident and migratory components of Mediterranean bluefin tuna have existed for almost as long as the period our dataset covers (6, 34, 35). Our findings do not suggest that Western and Central Mediterranean bluefin tuna are resident, rather that bluefin tuna that spawn at these locations are less likely to have originated from Atlantic spawning sites or the eastern Mediterranean. Tagging studies document well that bluefin tuna caught in the Western and Central Mediterranean during the spawning season migrate to the Atlantic (34, 61, 62). Studies tagging Norwegian or Eastern Mediterranean spawners are rare (35, 63) and thus it is possible that bluefin tuna from these locations may be more resident in the Mediterranean in some years, as isotope data across millennia suggest (37), while in other years contributing more to Atlantic spawning than Western and Central Mediterranean bluefin tuna. We find the latter most likely since migration patterns from Norway appear highly varied (63) and greater variation in spawning behaviors and mixing rates with the Western population are mechanisms that buffer genetic diversity loss.

There is a lack of knowledge on the contribution of each stock to spawning at Atlantic spawning sites, other than for the Slope Sea—where a mix of the two stocks was evident (33). We theorize increased spawning rates of Eastern Mediterranean and Norwegian bluefin tuna than Western and Central Mediterranean bluefin tuna in Atlantic spawning areas. A host of research supports increased complexity in bluefin tuna migrations and spawning than is currently recognized (6, 28, 33). For example, a proportion of bluefin tuna are genetically Mediterranean—but isotopically Western Atlantic (64), and a proportion of bluefin tuna may engage in skipped-spawning (65). Further work is required to assess whether Norwegian and Eastern Mediterranean bluefin tuna spawn in the Atlantic, while being more resident for the years that they spawn in the Mediterranean, including in the Black Sea as has been hypothesized (66, 67).

Depending on the season, the geographical and genetic distance between Mediterranean spawning sites could be minimal (25). Therefore, the high likelihood that spawning segregation is not always present in the Mediterranean could explain why the genetic differences between Western and Central vs. Eastern Mediterranean are not significant, despite that the admixture appears consistent in snap-shots across time. Due to the limited extent of these admixture patterns, caution should be taken when interpreting our findings and further research should be done to investigate the full extent and drivers of differences in spawning site use in Mediterranean bluefin tuna, whether they may be behavioral (migrational memory) (68) or genetic.

A Historical Demographic Decline and Genetic Erosion. We find genomic evidence that bluefin tuna began a slight but significant demographic decline by 1900, which is earlier than robust fisheries data became available (ca. 1960, (4). Currently, quantitative data recognize a demographic decline between 1960 and 2007, where Eastern bluefin tuna abundance and range declined by an estimated 70% and 46 to 53%, respectively (4, 5), followed by a recent recovery (13). Our demographic modeling suggests that the post-1960 losses represent only the most recent impacts of intensive exploitation. Supporting this, a host of evidence would point to exploitation being more intensive and impactful earlier than currently recognized. These include declines in prey and habitat suitability by the 1800s (16, 37), the highest tuna trap catch rates in history by the 1880s (40), a shift to fishing larger individuals by the early 1900s (39), and the seasonal, geographic, and gear expansion of fishing into the Atlantic by the early 1920s (3, 15). Together with findings on other species like Atlantic cod (*Gadus morhua*) (69) and herring (*Clupea harengus)* (16), preindustrial demographic declines appear to be common for commercial Atlantic marine fishes.

Since bluefin tuna fisheries seldom existed in the Western Atlantic until the 1950s (3), it is unlikely that Gulf of Mexico bluefin tuna declined to the same extent as the Mediterranean, as our data suggest. Similar demographic histories for both populations over the past millennia could be due to the limitation of the measure of effective population size, which is affected by gene flow between populations (33, 70). Effective population size thus cannot be directly interpreted as biomass for each population but rather the demography of the species (71). Given that bluefin tuna demography appeared stable across hundreds of years prior to the 1800s, we suggest that demographic changes were caused by novel challenges like increased fishing effort, causing more dramatic fluctuations in biomass than is normally reflected by climate and other factors (6, 38, 72).

A widely accepted consequence of biomass declines is genetic bottlenecks, in which genetic diversity decreases due to a loss of alleles and increase in inbreeding. This has been well documented for other taxa such as marine seabirds and marine mammals (23, 42–44), but evidence has been scarce for fish populations (but see ref. 73). Our work suggests that marine fishes are not immune to genetic erosion following the finding of decreases in heterozygosity and nucleotide diversity, corresponding to a period of overexploitation and demographic decline by the early 1900 s. The only other whole genome aDNA analysis of marine fishes suggested genetic diversity retention in the overexploited Atlantic cod (45)—though this study did not analyze samples older than the year 1900—and genetic diversity loss in Atlantic herring (73). Both genetic stability (46, 47, 50, 74–76) and erosion (48, 77, 78) have been observed using fewer SNPs, microsatellites, or mitochondrial DNA. Findings of genetic diversity loss do not suggest that bluefin tuna's or other fish populations with similar demographic histories are at risk of extinction. The genomic changes we observe are relatively small and a host of information evidence that bluefin tuna populations are rebounding (9–11, 13).

It is likely that a combination of bluefin tuna ecological features buffer against losses in genetic diversity such as high population connectivity, large population size, and a long life cycle which promotes heavily overlapping generations (25, 79). Theoretically, each of these features limit the effect of genetic drift (80, 81), such that a larger number of generations would need to have elapsed in order to observe changes in heterozygosity as a result of biomass declines. This may explain why the decrease in heterozygosity and nucleotide diversity we observed between ancient and modern bluefin tuna was slight (ca. 1 to 1.5% sites), though significant. Dictating the degree of genetic diversity loss in modern samples, we find that inbreeding extents (fraction of the genome in runs of homozygosity) differ between modern spawning areas, which corroborate patterns of admixture i.e. Eastern Mediterranean bluefin tuna had a significantly lower inbreeding extent than Western Mediterranean bluefin tuna, which we hypothesize is due to a greater contribution of Western Atlantic gene flow to the Eastern Mediterranean.

There is concern that the Western Atlantic population is at genetic risk due to a perceived greater population decline coupled with a strong recovery in the Mediterranean population (13, 33). Our work suggests that the Western Atlantic and Mediterranean populations do not significantly differ in inbreeding extent or nucleotide diversity. Overall, population-specific F_{ST} indicated that the Gulf of Mexico is more heterogeneous than the Mediterranean spawning sites, as has been suggested previously (33), which we theorize is because the Western Atlantic population is more ancestral. We agree with (33) that an increasing number of east to west migrants (82) may have the potential to erode differences between the Western and Eastern stocks, but our results suggest that the mixing of the populations in Atlantic spawning areas has been a phenomenon for millennia.

Approach and Limitations. Due to ancient sample availability and postmortem DNA damage, we here opted to study a high-quality yet relatively small dataset in terms of sample size and SNPs. This is a vast improvement on studies that focused on only a handful of SNPs, but could still be improved in further studies that allow for deeper sequencing and an improved genomic reference(s). First, we cannot exclude the possibility that reference bias (83) may have impacted our admixture results but we consider this to be unlikely given that elevated levels of Gulf of Mexico admixture in the eastern Mediterranean samples occurred regardless of sample age and read depth. Second, we cannot rule out that challenges in ancient sample preservation and sequencing biases have not impacted patterns of genetic diversity differences between ancient and modern samples. However, these differences remained after filtering out sites potentially impacted by DNA damage and when increasing the depth and quality of genotypes even further. Moreover, we filtered loci to the extent that lower coverage samples did not have excesses of homozygosity, avoiding this common problem in sequence datasets (84).

In addition, we filtered SNPs by F_{ST} to remove highly conserved or erroneous sites when analyzing ancient samples, as these sites—likely to be under balancing selection—have been shown to reduce the appearance of population differentiation (76, 77) (*SI Appendix*, Fig. S4). Low F_{ST} sites are likely to maintain genetic diversity in marine populations (85); when including these loci, we found that proportions of heterozygosity loss were lower over time (*SI Appendix*, Fig. S8). We consider that the inclusion of highly conserved loci would have hindered our observations and is not always appropriate for detecting changes in datasets with low levels of population divergence and ancient DNA damage. On the other hand, certain analyses, e.g., nucleotide diversity required sufficient window SNP density such that a conservative approach was not possible with our dataset where we had to allow missing data into analyses. The variety of filtering methods taken provide support that patterns observed are likely to be true and appear regardless of approach.

Any study investigating effective population size should reiterate that its relationship with census size is complex for fishes such as bluefin tuna with very large census sizes (81). Moreover, effective population size estimates are influenced by many factors (71, 86), chiefly gene flow—which in the case of bluefin tuna appears high. Due to a lack of preindustrial commercial exploitation in the Western Atlantic, we propose that gene flow from the Western stock buffered the demographic decline we observed in bluefin tuna by 1900. Caution should be taken in that the extent of N_e decline may not corroborate the same extent in biomass decline because of aforementioned population structure-related (and technical) biases despite our attempts to avoid these through high-quality loci filtering and use of a dataset weak in population structure following (87). In addition, the timing of the decline is biased by the chosen generation length. In this study, we used three alternatives to be conservative, but their consistency and relevance over time is unknown. We find it unlikely that population structure biased our GONE results, as can be an issue for some species at low effective population sizes not observed here [ca. 1000s, (87)], due to limited population structure in bluefin tuna ($F_{ST} < 0.002$) that resulted in near-identical trajectories regardless of samples used. We followed best practices (87) to avoid this bias as much as possible: using a dataset where populations were not structurally separate (*SI Appendix*, Fig. S4) and removing outputs for the past ca. 40 y (ca. 4 generations). Limitation of the method, precluding the opportunity to realize

effective population sizes for recent generations should be explored to capture the full extent of the demographic decline and contextualize the recent recovery.

Our lack of a high-quality annotated reference precluded the opportunity to assess the location of SNPs which vary in space or time and their function. Future studies should assess gene ontology and assess mechanisms underlying these polymorphisms. For example, they may represent polygenic or epistatic, global adaptation (80, 88–91), even if they are at low-F_{ST} differences in space or time.

Aided by ancient DNA, we provided directions for future research by indicating that the spawning, recovery, and genetics of bluefin tuna are likely to be more complex than currently recognized. Improved genomic resources are almost certain to facilitate improved understandings on the scale of impacts and diversity of populations, especially in cases such as bluefin tuna where population differentiation is low. Our findings call for additional analyses on temporal analyses of bluefin tuna and other marine fishes, using high-quality annotated reference genomes, larger sample sizes, and coverage. We show how ancient DNA has the potential to aid marine management and conservation plans by providing perspectives of when demographic declines began to revise recovery targets and ways to measure population sustainability, depending on what genetic diversity is lost and its functional implications.

Methods and Materials

Sample Collection. We collected samples of modern bluefin tuna for analysis as follows: contemporary larvae or young-of-the-year specimens (Gulf of Mexico, Western Mediterranean - Balearic Islands, Central Mediterranean - Sicily, Eastern Mediterranean - Levantine Sea, n = 40, Table 1; *SI Appendix*, Table S1) were collected from each of the major bluefin tuna spawning sites between 2013 and 2018 (Fig. 1, Table 1 and *SI Appendix*, Table S1). In addition, we collected and analyzed adult bluefin tuna (n = 10) caught off the Norwegian coast in 2018 that do not represent a spawning site and could have originated from any spawning area. For further sample details, see *SI Appendix*. Larvae or muscle tissue samples from each specimen were preserved in 96% ethanol and stored at −20 °C until extraction.

Ancient samples included archived vertebrae (n = 12; Table 1) which were retrieved from the Massimo Sella Archive (50) and pertained to two tuna-trap catches of 1941 (Istanbul, Türkiye) and 1925 (Zliten, Libya: Table 1 and Fig. 1*A*). Ancient samples also included archaeological vertebrae (n = 32, Table 1) retrieved from several Norwegian and Mediterranean excavations throughout the past five millennia (Fig. 1*A*) including 1750 to 1850 (Marseille Harbour, Marseille, France), 1600 to 1800 (Pedras de Fogu, Sassari, Italy), 900 to 1,200 (Sicily, Italy), 800 to 1,300 (Yenikapi, Istanbul, Türkiye), and 3000 BCE (Jortveit, Norway). See *SI Appendix* for more details on ancient samples and their dating.

Ancient DNA Extraction. The majority of archaeological and historical bluefin tuna samples underwent ancient DNA (aDNA) extraction in dedicated, sterile, PCR-free conditions at the Ancient DNA Laboratory of the Department of Cultural Heritage (University of Bologna, Ravenna Campus, Italy). The two ancient Norwegian samples were processed in a dedicated aDNA laboratory at the University of Oslo as detailed in (92). Samples processed in the Ancient DNA Lab followed strict criteria for aDNA analysis (93, 94). The outer surfaces of bones were cleaned with a ca. 20% sodium hypochlorite (bleach) solution and left to air-dry for 10 min. Specimens were then exposed to UV light (254 nm) for 15 min on each side before drilling to remove an outer layer (ca. 2 mm) of material. Between 100 and 350 mg of bone powder was then collected by drilling at the same position where the outer layer had been removed. Care was taken to avoid overheating specimens by drilling at slow speeds with diamond-tipped drill-bits.

Isolation of aDNA was performed using a modified version of Dabney et al. (95, 96). Briefly, 100 to 300 mg bone powder from each sample was predigested (97) for 20 min at 37 °C in 1 to 3 mL digestion buffer containing EDTA (0.45 M, pH 8.0) and proteinase K (0.25 mg/mL). Lysates were then discarded before samples were fully digested overnight in the same conditions. Once digested, lysates were combined with 10 mL of binding buffer (PB buffer, Qiagen, Germany) and bound to the High Pure Viral Nucleic Acid Large Volume silica spin columns (Roche, Basel, Switzerland) by centrifugation. Membrane-bound aDNA was then washed twice with 720 μL PE buffer (Qiagen), before elution in 30 μL of EB buffer (Qiagen). The total DNA obtained from each extraction was quantified using the Qubit dsDNA HS (High Sensitivity) Assay Kit (Thermo Fisher Scientific, USA). Negative controls employed in each batch of samples extracted indicated an undetectable level of contamination (<500 pg/mL). Extractions were then stored at −20 °C until library preparation.

Modern DNA Extraction. Modern spawning site specimens were extracted at the GenoDREAM laboratory of the Department of Biological, Geological and Environmental Sciences (University of Bologna, Ravenna Campus, Italy). Modern Norwegian samples were collected by the Norwegian Institute of Marine Research (IMR), freeze-dried and powdered at IMR facilities, and extracted in the modern DNA isolation laboratories at the Center for Ecological and Evolutionary Synthesis, University of Oslo, Norway) as detailed in (92). Modern spawning site samples were processed using a modified salt-based extraction protocol (98) using SSTNE extraction buffer (99) and treated with RNase (Qiagen) to remove residual RNA. After isolation, the total DNA obtained from each extraction was quantified using the Qubit dsDNA BR Assay Kit (Thermo Fisher Scientific, USA). Negative controls employed for each batch of samples extracted confirmed an undetectable level of contamination. Samples were diluted to 10 ng/μL. Prior to library preparation, 100 μL of DNA extracted from each modern sample was sheared to maximum sizes of 500 bp using a Bioruptor Pico sonicator (Diagenode) with the settings: Medium 30 on/90 off for 10 min. Samples were precipitated using isopropanol, following a procedure from Qiagen (FAQ-ID-2953). Fragment lengths were confirmed by agarose gel electrophoresis and total DNA was requantified using Qubit before precipitates were stored at −20 °C until library preparation.

DNA Library Preparation and Sequencing. With exception to the Norwegian samples which were prepared as detailed in (92), single-stranded libraries were built for both ancient and modern samples using the Santa Cruz Reaction (SCR) method (100) from 10 to 20 μL of DNA, up to a maximum input of 150 ng. Prior to indexing, aDNA libraries were prepared in sterile conditions at the Ancient DNA Laboratory of the Department of Cultural Heritage, separate from those facilities used to prepare modern libraries. Library quality and the non-amplification of controls were confirmed using qPCR following the SCR method, which indicated the number of cycles required for indexing and inhibited samples to be discarded. Ligated DNA was double-indexed with sample-specific 6 bp indexes by amplification using 2X Amplitaq Gold 360 MM (Thermo Fisher Scientific, USA), and 25 to 50 μM of each index for 10 to 14 cycles (2 min at 95 °C, cycles of 30 s at 95 °C, 30 s at 60 °C, and 70 s at 72 °C with a final extension of 10 min at 72 °C). Amplified products were cleaned by using AMPure XP beads (Agencourt) at a 1:1.2 ratio, eluted in 25 μL in EB buffer, and quantified using a Bioanalyzer 2100 (Agilent Technologies). All libraries were screened to explore DNA preservation and library clonality by sequencing ca. 1 million reads per sample on the Illumina HiSeq X, 2,500 or 4,000 platforms (100 bp paired-end). Libraries were then resequenced (150 bp paired-end) on the HiSeq 4000 or NovaSeq S4 Illumina platform, to the final sequencing depths reported. Sequencing and demultiplexing (allowing zero mismatches in the index tags) were performed at the Norwegian Sequencing Center (Oslo, Norway) and Macrogen facilities (Seoul, South Korea/Amsterdam, Netherlands) with care taken to avoid batch effects by pooling varied combinations of samples (*SI Appendix*, Table S1).

Reference Assembly Improvement. Since a chromosome-level assembly was not available at the time of analyses, we improved a draft assembly. The highly scaffolded draft *Thunnus thynnus* genome assembly [(101), NCBI BioProject: PRJNA408269] was mapped against the chromosome-scale assembly of yellowfin tuna (*Thunnus albacares*, fThuAlb1.1, NCBI accession: GCA_914725855.1). Scaffolds were mapped using BBMap (102) with the asm10 setting which successfully mapped 102,121 out of 103,645 (98.5%) scaffolds to yellowfin tuna chromosomes. Scaffolds were then binned into the 24 yellowfin tuna chromosomes by placing 200 N's between them, resulting in a 768 Mb pseudochromosome assembly. Nonmapped (unplaced) scaffolds were excluded from analyses.

Data Processing and Filtering. Due to initial read lengths being longer in modern Norwegian samples (ca. 160 bp, *SI Appendix*, Table S1), because DNA was not sonicated as modern Gulf of Mexico and Mediterranean samples, we first

trimmed Norwegian reads to 100 bp. Our aim was to produce a dataset that was technically comparable and avoid one sample group having sequence length or depth much greater than others. Raw Norwegian sequences were trimmed using Trimmomatic v.0.39 (103), using the settings clip = 100, headclip = 5. Details of average sequence lengths across all samples can be found in *SI Appendix*, Table S1.

Ancient and modern reads were processed by using PALEOMIX (104) which is a set of pipelines and tools designed to aid the rapid processing of high-throughput ancient sequencing data. Forward and reverse reads were collapsed in PALEOMIX with AdapterRemoval v1.5 (105) and aligned to our pseudochromosome bluefin tuna reference using BWA mem (102). Only reads that had a minimum length of 25 bp were aligned, and only with a minimum quality score (MapQ) of 30 i.e. a 0.1% chance each read was misaligned were used for subsequent analyses. Ancient DNA damage patterns were investigated by using mapDamage v.2.0.6 (106). Finally, we removed all clipped reads (or pairs of reads for which one read was clipped) and all duplicate reads (Picard Tools v. 1.96) and then realigned indels using GATK v. 3.7 IndelRealigner (107). To reduce the influence of postmortem DNA damage that can be a problem for ancient DNA datasets, we studied damage patterns (*SI Appendix*, Fig. S1) and trimmed 3 bp from all ancient mapped reads using the TrimBam function of bamUtil v.1.0.6 (108) and reindexed using samtools v1.7 (109). This reduced the frequency of deamination to below 5% in all reads. Average read-depths were 9.9 and 11.9 fold coverage for ancient and modern samples, respectively.

We used GATK to jointly call SNPs (GATK HaplotypeCaller and GenotypeGVCFs) for ancient and modern samples using default settings, allowing a maximum of three alternative alleles. We filtered SNPs using conservative established approaches. First, SNPs were hard-filtered for strand bias (FS and SOR), mapping quality (MQ), quality by depth (QD), nonpolymorphism (AC) using BCFTOOLS v. 1.6 with settings filter --i "FS>60.0 || SOR>4 || MQ<30 || QD<2.0 || AC==0 || AC==AN." Then, we removed indels and retained only, biallelic SNPs using VCFtools v.0.1.16 (110) with settings --remove-indels --min-alleles 2 --max-alleles 2.

VCFtools was used to filter for genotype quality (GQ), depth (minDP and max-meanDP), and minor allele frequency (MAF). A minimum GQ of 20 was applied to remove low confidence genotypes expected due to aDNA characteristics such as postmortem damage and highly variable coverage across the genome. SNPs present in genomic regions where reads preferentially mapped more than twice the average (likely repetitive regions) were removed using a max-meanDP filter set to 30; ca. double the coverage of the majority of our highest coverage samples. A minDP filter of 5 was used, to provide confidence that homozygous loci were not artifacts of insufficient coverage. MAF filters were used to remove doubletons which may represent poor sequencing or DNA quality, and set depending on the number of samples present in multisample VCFs i.e --maf 0.05 or 0.02 if using modern (n = 50) or modern and ancient (n = 95) samples, respectively. No missing data were tolerated for analyses (--missing-data 1). Finally, to retain sufficient loci with this conservative approach, three ancient samples were dropped from analyses due to low coverage <6X (IST_913C_01, IST_913C_02, and PF_1618C_23, *SI Appendix*, Table S1).

We excluded loci that were out of Hardy–Weinberg equilibrium (HWE) due to the possibility that highly hetero- or homozygous loci represent nonbiological sequencing artifacts, or signatures of introgression that could be present in few individuals (e.g., ref. 33) and may bias analyses with small numbers of samples. We opted to remove loci if they yielded a *P*-value <0.001 following a site-specific exact test across all samples as implemented in VCFtools. The trade-off with this filter is that we will not observe highly variable sites which may be signatures of selection however since recently no large effect loci have been observed in bluefin tuna (33), we assumed that loci that were highly hetero- or homozygous are more likely nonbiological sequencing artifacts. We illustrate the effect of HWE filters in the supplementary (*SI Appendix*, Figs. S5 and S6).

Due to the possibility that multiple ancient bones were sequenced from the same individual, or that modern tissues were sampled from closely related individuals that might bias analyses, we tested pairwise relatedness between samples in VCFtools using --relatedness2. This resulted in the removal of two ancient specimens from analyses (CDM_10C_07 and CDM_10C_11) due to their kinship coefficient >0.35 i.e. duplicate/twin with CDM_10_04. The modern sample CYPR-LS-331 was removed for the same reason due to its close-kinship >0.35 with CYPR-LS-330.

Overall, these filters produced final datasets across the 768 Mb bluefin reference genome of 39 modern spawning site individuals with 664,522 loci and combined ancient and modern datasets of 90 individuals with 30,264 loci. In summary, these datasets differ in the number of SNPs and that the number of erroneous sites may be higher for ancient individuals, subject to DNA damage.

To remove highly conserved or erroneous sites from the dataset which did not vary consistently over time or space and that therefore may have clouded inference of spatiotemporal variability, we assessed F_{ST} per site and filtered out loci if their F_{ST} values were <0 across all spatiotemporal sample groups. Setting the filtering threshold at <0 F_{ST} was an arbitrary but conservative approach, removing sites that were on average more variable within groups than between them. This approach was preferred to filtering and analyzing "outlier loci" as is common practice for fishes with low levels of population differentiation e.g. (111, 112) since population differentiation or adaptation in bluefin tuna is most likely not driven by large effect loci (33), and therefore, these loci were perceived as errors, likely not-population defining. Therefore, our aim was to retain relatively low F_{ST} but consistently (between time periods) variable sites in the dataset. F_{ST} was estimated in VCFtools with the commonly used --weir-fst-pop function (113, 114) with default settings. This function calculated per-locus pairwise F_{ST} (51), between all spatiotemporal groups. A distribution of F_{ST} per locus from the calculations can be observed in the supplementary (*SI Appendix*, Fig. S17). VCFtools was also used as the means to filter out loci using the --position function. F_{ST} filtering resulted in 17,741 loci of the 30,264 loci remaining.

Population Structure and Admixture. SNPs were pruned (–indep-pairwise 50 5 0.2) for linkage disequilibrium using PLINK v1.90b6.21 (115) following (116). Therefore, analyses were performed on two datasets: one pruned modern dataset of 386,963 loci, and one filtered, pruned modern and ancient dataset of 12,838 loci. A principal component analysis (PCA) was performed using EIGENSOFT v.5.1 (117). PCA is a method free of HWE assumptions but is open to technical bias (118); therefore, we opted to avoid overinterpreting these results. We reran analyses and included sites previously removed by our F_{ST} filter threshold (F_{ST} >0) and reran PCAs on 27,882 loci to explore the need for filtering loci by F_{ST} to observe and infer correct population structure.

Population structure was also evaluated on the same datasets using STRUCTURE v.2.3.4 (119), which implements a Bayesian clustering method assuming HWE to identify the most likely number of populations (K). We followed the Evanno et al. (120) method, and thus, we carried out 10 runs per each value of K ranging from 1 to 5. Runs used the admixture models and assumed correlated allele frequencies without locprior. Each run used 10,000 burn-in and 50,000 Markov Chain Monte Carlo replicates. We estimated the ad hoc statistic ΔK in order to infer the most likely number of populations (2 to 5) using STRUCTURE HARVESTER (121), given that this method is not able to assess the likelihood of K = 1. CLUMPAK (122) was used to merge the 10 runs from the most probable K, which reported similarity scores >95%. Pairwise distances between modern spawning site samples were calculated with Nei's estimator of F_{ST} (123) as implemented in the hierfstat R package, using 1,000 permutations to calculate p-values, which were judged for significance under the FDR approach at the 5% level.

Genetic Diversity Statistics. Genetic diversity statistics were calculated using the filtered, dataset of 90 modern and ancient samples at 17,741 loci. Heterozygosity (proportion of sites) was calculated for each individual using VCFtools --het. We removed transition sites (C > T and G > A SNPs) which may be affected by postmortem taphonomic degradation and reran the heterozygosity analysis on the remaining 5,822 loci, which revealed our findings hold true irrespective of the potential DNA damage. To confirm our results were indicative of genome-wide patterns, we removed the per-site F_{ST} filter and allowed 10% missing data (using VCFtools --missing-data 0.9) into the dataset to produce 2,890,241 loci and reran analyses which revealed that these patterns appear to be genome-wide. The same dataset, reprocessed using BCFTOOLS to include nonvariant sites, was used to calculate nucleotide diversity (pi). Nucleotide diversity (pi) was calculated for each sample group per 50 kb (-w 50,000 -m 10) windows using the script popgenWindows.py (https://github.com/simonhmartin/genomics_general). As a proxy for inbreeding extent, runs of homozygosity (RoH) were analyzed for the modern spawning site samples using a filtered unpruned dataset of 664,522 loci following (124). ROHs were calculated using PLINK across 200 kb windows following (16) with

the following settings homozyg-snp 20 --homozyg-kb 200 --homozyg-density 20 --homozyg-gap 1,000 --homozyg-window-snp 20 --homozyg-window-het 2 --homozyg-window-missing 5 --homozyg-window-threshold 0.05. Wilcoxon rank-sum tests were performed in R to judge the statistical significance of summary statistic differentiation between sample groups, at the 5% level.

Finally, because challenges in identifying true heterozygous loci in low-coverage and ancient DNA datasets can lead to biases in heterozygosity estimates (84), we refiltered the main (17,741 loci) dataset using VCFtools to ensure loci were supported by at least 10 reads (--minDP 10) and we increased the genotype quality filter (minimum GQ) from 20 to 25, by allowing missing data (--missing-data 0.9). We reran VCFtools --het on this high-quality dataset of 334,783 loci. We explored the relationship between average sample depth and homozygosity for this dataset and the main dataset using linear regression (*SI Appendix*, Fig. S16).

Effective Population Size. We reconstructed historical effective population size (N_e) using GONE v.1 (125). GONE uses linkage disequilibrium (LD) to estimate N_e for the previous 200 generations. GONE was run on the unpruned filtered dataset of modern spawning site samples comprising 664,522 loci, grouped by western or eastern stock (Gulf of Mexico, n = 10; Mediterranean n = 39). We converted GONE outputs of N_e estimates per generation number to years (BCE/CE) using a generation length of between 10 and 16 y, with 13 y being the most widely accepted following (81) and https://fishbase.se. We discarded estimates of the previous 4 generations (ca. last 50 y) as these yielded extremely low N_e estimates (ca. 15 to 20 k), likely as a function of methodological limitations (86). We reran analyses after removing the maf filter which resulted in similar trajectories and tested for the effect of sample size by grouping Mediterranean samples by spawning site (n = 9 or 10), which yielded near-identical N_e trajectories over time as when analyzed pooled (*SI Appendix*, Fig. S14).

Outlier Analyses. To assess the impact of HWE filters and investigate outliers across the genome which we hypothesized would include patterns of introgression recently observed in bluefin tuna (33), we used the SNP-based outlier detection method with the lowest false positive rates which detects outlier loci using allele frequencies: pcadapt (126). pcadapt does not require sample groups to be defined. We ascertained population structure via PCA and determined outlier loci as those excessively correlated with two (K = 2) ordination axes. pcadapt was run in R using the unpruned HWE-filtered and non-HWE-filtered modern spawning site datasets of 39 individuals and 664,522 and 1,106,859 loci, respectively.

To better understand F_{ST} distribution across the genome between ancient and modern samples and the drivers of temporal genetic diversity changes, we assessed F_{ST} outliers in OutFLANK v.02 (127) using the unpruned filtered modern and ancient dataset of 90 individuals and 30,264 SNPs. OutFLANK was run in R using suggested settings (LeftTrimFraction = 0.05, RightTrimFraction = 0.05) and a false discovery rate (FDR) of ≤5% (127). OutFLANK accounts for sampling error and nonindependence between sample groups provided a priori while inferring the F_{ST} distribution of loci and fitting a χ^2 model to the center of the distribution.

Data, Materials, and Software Availability. The raw genomic sequence data reported in this article are available at the NCBI https://dataview.ncbi.nlm.nih.gov/object/PRJNA1238330 (128). The genomic reference used to analyze the data is available at https://www.ncbi.nlm.nih.gov/bioproject/PRJNA408269 (129). All metadata are included in the manuscript and/or supporting information.

ACKNOWLEDGMENTS. This work is a contribution to the https://tunaarchaeology.org and was funded by the European Union Horizon 2020 Grant Number 813383 as part of the Marie Skłodowska-Curie Actions Innovative Training Network SeaChanges. We are grateful to Sara De Fanti and Anisa Ribani for laboratory support and to Paolo Abondio and Shripathi Bhat for bioinformatics advice. We would like to thank the National Oceanic and Atmospheric Administration Restore Project that aided the collection of western Atlantic samples and the Institute of Marine Research (Norway) for access to modern Norwegian samples.

Author affiliations: [a]Section for Marine Biology, Norwegian Institute of Water Research, Oslo 0579, Norway; [b]Department of Biological, Geological and Environmental Sciences, University of Bologna, Ravenna 48123, Italy; [c]Centre for Ecology and Evolutionary Synthesis, University of Oslo, Oslo 0371, Norway; [d]Norges fiskerihøgskole, University of Tromsø Arctic University of Norway, Tromsø 9037, Norway; [e]Aquastudio Research Institute, Messina 98121, Italy; [f]Cooperative Institute for Marine and Atmospheric Studies, University of Miami, Miami, FL 33146; [g]National Oceanic and Atmospheric Administration Fisheries, Populations and Ecosystems Monitoring Division, Miami, FL 33149; [h]Faculty of Veterinary Medicine, Muğla Sıtkı Kocman University, Milas 48100, Türkiye; [i]Consejo Superior de Investigaciones Científicas, Institució Milà, Barcelona 08001, Spain; [j]CEPAM, CNRS, Université Côte d'Azur, Nice 7264, France; [k]Archéologie des Sociétés Méditerranéennes, CNRS, Université Paul Valéry, Montpellier 34199, France; [l]Stavanger Maritime Museum, Stavanger 4005, Norway; [m]Museum of Cultural History, University of Oslo, Oslo 0164, Norway; [n]Department of Cultural Heritage, University of Bologna, Ravenna 48121, Italy; and [o]Department of Anthropology, University of British Columbia, Vancouver 6303, Canada

1. A. Kuparinen, J. A. Hutchings, Consequences of fisheries-induced evolution for population productivity and recovery potential. *Proc. Biol. Sci.* **279**, 2571–2579 (2012).
2. C. M. Duarte *et al.*, Rebuilding marine life. *Nature* **580**, 39–51 (2020).
3. C. E. Porch, S. Bonhommeau, G. A. Diaz, A. Haritz, G. Melvin, "The journey fromoverfishing to sustainability for Atlantic bluefin tuna, Thunnus thynnus" in *Future BluefinTunas: Ecology, Fisheries Management, and Conservation*, B. A. Block, Ed. (JohnsHopkins University Press, 2019), pp. 3–44.
4. B. R. MacKenzie, H. Mosegaard, A. A. Rosenberg, Impending collapse of bluefin tuna in the northeast Atlantic and Mediterranean. *Conserv. Lett.* **2**, 26–35 (2009).
5. ICCATI, Report of the 2006 Atlantic bluefin tuna stock assessment session. *Col. Vol. Sci. Pap.* **60**, 652–880 (2007).
6. J.-M. Fromentin, Lessons from the past: Investigating historical data from bluefin tuna fisheries. *Fish Fish* **10**, 197–216 (2009).
7. M. R. Siskey, M. J. Wilberg, R. J. Allman, B. K. Barnett, D. H. Secor, Forty years of fishing: Changes in age structure and stock mixing in northwestern Atlantic bluefin tuna (Thunnus thynnus) associated with size-selective and long-term exploitation. *ICES J. Mar. Sci.* **73**, 2518–2528 (2016).
8. B. Worm, D. P. Tittensor, Range contraction in large pelagic predators. *Proc. Natl. Acad. Sci. U.S.A.* **108**, 11942–11947 (2011).
9. L. Nøttestad, E. Boge, K. Ferter, The comeback of Atlantic bluefin tuna (Thunnus thynnus) to Norwegian waters. *Fish. Res.* **231**, 105689 (2020).
10. T. W. Horton *et al.*, Evidence of increased occurrence of Atlantic bluefin tuna in territorial waters of the United Kingdom and Ireland. *ICES J. Mar. Sci.* **78**, 1672–1683 (2021), 10.1093/icesjms/fsab039.
11. A. Di Natale, S. Tensek, A. P. García, Is the bluefin tuna slowly returning to the Black Sea? Recent evidences *Col. Vol. Sci. Pap. ICCAT* **75**, 1261–1277 (2019).
12. C. Carrano *et al.*, asap stock assessment of The Eastern Atlantic and Mediterranean bluefin tuna. *Collect. Sci.* **79**, 551–586 (2022), https://www.iccat.int/Documents/CVSP/CV079_2022/n_3/CV079030551.pdf.
13. ICCAT, *Report of the 2020 Second ICCAT Intersessional Meeting of The Bluefin Tuna Species Group. Online, 20-28 July 2020. Second BFT Intersessional Meeting - Online 2020* (2020).
14. M. J. Juan-Jordá *et al.*, Seventy years of tunas, billfishes, and sharks as sentinels of global ocean health. *Science* **378**, eabj0211 (2022).
15. A. J. Andrews *et al.*, Exploitation history of Atlantic bluefin tuna in the eastern Atlantic and Mediterranean–insights from ancient bones. *ICES J. Mar. Sci.* **79**, 247–262 (2022).
16. L. M. Atmore *et al.*, Population dynamics of baltic herring since the viking age revealed by ancient DNA and genomics. *Proc. Natl. Acad. Sci. U.S.A.* **119**, e2208703119 (2022).
17. J. B. Jackson *et al.*, Historical overfishing and the recent collapse of coastal ecosystems. *Science* **293**, 629–637 (2001).
18. H. K. Lotze, R. Hoffmann, J. Erlandson, *Lessons from Historical Ecology and Management in The Sea, Volume 19: Ecosystem-Based Management* (Harvard University Press, 2014).
19. E. J. Guiry *et al.*, Early evidence for historical overfishing in the Gulf of Mexico. *Sci. Adv.* **7**, eabh2525 (2021).
20. K. Schwerdtner Máñez *et al.*, The future of the oceans past: Towards a global marine historical research initiative. *PLoS ONE* **9**, e101466 (2014).
21. G. L. Britten, M. Dowd, B. Worm, Changing recruitment capacity in global fish stocks. *Proc. Natl. Acad. Sci. U.S.A.* **113**, 134–139 (2016).
22. E. L. Jensen *et al.*, Ancient and historical DNA in conservation policy. *Trends Ecol. Evol.* **37**, 420–429 (2022).
23. M. Kardos *et al.*, The crucial role of genome-wide genetic variation in conservation. *Proc. Natl. Acad. Sci. U.S.A.* **118**, e2104642118 (2021).
24. ICCATI, *Report of the Standing Committee on Research and Statistics (SCRS) (Hybrid / Madrid (Spain) – 23-27 September 2024). International Commission for the Conservation of Atlantic Tunas*. (2024). https://www.ICCATiccat.int/Documents/BienRep/REP_EN_24-25-I-2.pdf
25. C. Piccinetti, A. Di Natale, P. Arena, Eastern bluefin tuna (Thunnus thynnus, L.) reproduction and reproductive areas and season. *Col. Vol. Sci. Pap. ICCAT* **69**, 891–912 (2013).
26. G. N. Puncher *et al.*, Spatial dynamics and mixing of bluefin tuna in the Atlantic Ocean and Mediterranean Sea revealed using next-generation sequencing. *Mol. Ecol. Resour.* **18**, 620–638 (2018).
27. N. Rodríguez-Ezpeleta *et al.*, Determining natal origin for improved management of Atlantic bluefin tuna. *Front. Ecol. Environ.* **17**, 439–444 (2019).
28. D. E. Richardson *et al.*, Discovery of a spawning ground reveals diverse migration strategies in Atlantic bluefin tuna (Thunnus thynnus). *Proc. Natl. Acad. Sci. U.S.A.* **113**, 3299–3304 (2016).
29. J. L. Cort, P. Abaunza, "The Present State of Traps and Fisheries Research in the Strait of Gibraltar" in *The Bluefin Tuna Fishery in the Bay of Biscay: Its Relationship with the Crisis of Catches of Large Specimens in the East Atlantic Fisheries from the 1960s*, J. L. Cort, P. Abaunza, Eds. (Springer International Publishing, 2019), pp. 37–78.
30. R. M. Dickhut *et al.*, Atlantic bluefin tuna (Thunnus thynnus) population dynamics delineated by organochlorine tracers. *Environ. Sci. Technol.* **43**, 8522–8527 (2009).

31. J. M. Rodriguez, C. Johnstone, D. Lozano-Peral, Evidence of Atlantic bluefin tuna spawning in the Bay of Biscay, north–eastern Atlantic. *J. Fish Biol.* **99**, 964–969 (2021).
32. C. M. Hernández *et al.*, Support for the Slope Sea as a major spawning ground for Atlantic bluefin tuna: Evidence from larval abundance, growth rates, and particle-tracking simulations. *Can. J. Fish. Aquat. Sci.* **79**, 814–824 (2022).
33. N. Díaz-Arce *et al.*, Unidirectional trans-Atlantic gene flow and a mixed spawning area shape the genetic connectivity of Atlantic bluefin tuna. *Mol. Ecol.* **118**, e2104642118 (2023), 10.1111/mec.17188.
34. P. Cermeño *et al.*, Electronic tagging of Atlantic bluefin tuna (Thunnus thynnus, L.) reveals habitat use and behaviors in the Mediterranean Sea. *PLoS ONE* **10**, e0116638 (2015).
35. G. De Metrio *et al.*, Joint Turkish-Italian research in the Eastern Mediterranean: Bluefin tuna tagging with pop-up satellite tags. *Col. Vol. Sci. Pap. ICCAT* **56**, 1163–1167 (2004).
36. A. Natale, A. Mangano, C. C. Piccinetti, E. Ciavaglia, A. Celona. Bluefin tuna (Thunnus Thynnus l.) line fisheries in the Italian seas. Old and recent data. *Collect. Vol. Sci. Pap. ICCAT* **58**, 1285–1295 (2005).
37. A. J. Andrews *et al.*, Exploitation shifted trophic ecology and habitat preferences of Mediterranean and Black Sea bluefin tuna over centuries. *Fish Fish* **24**, 1067–1083 (2023).
38. C. Ravier, J.-M. Fromentin, Long-term fluctuations in the eastern Atlantic and Mediterranean bluefin tuna population. *ICES J. Mar. Sci.* **58**, 1299–1317 (2001).
39. A. J. Andrews, Vertebrae reveal industrial-era increases in Atlantic bluefin tuna catch-at-size and juvenile growth. *ICES J. Mar. Sci.* **80**, 836–847 (2023).
40. A. Pagá Garcia *et al.*, Report on revised trap data recovered by iccat gbyp from phase 1 to phase 6. *Col. Vol. Sci. Pap. ICCAT7.* **3**, 2074–2098 (2017).
41. T. Oosting *et al.*, Unlocking the potential of ancient fish DNA in the genomic era. *Evol. Appl.* **12**, 1513–1522 (2019).
42. D. Díez-Del-Molino, F. Sánchez-Barreiro, I. Barnes, M. T. P. Gilbert, L. Dalén, Quantifying temporal genomic erosion in endangered species. *Trends Ecol. Evol.* **33**, 176–185 (2018).
43. O. Kersten *et al.*, Hybridization of Atlantic puffins in the Arctic coincides with 20th-century climate change. *Sci. Adv.* **9**, eadh1407 (2023).
44. M. Louis *et al.*, Ancient dolphin genomes reveal rapid repeated adaptation to coastal waters. *Nat. Commun.* **14**, 4020 (2023).
45. M. L. Pinsky *et al.*, Genomic stability through time despite decades of exploitation in cod on both sides of the Atlantic. *Proc. Natl. Acad. Sci. U.S.A.* **118**, e2025453118 (2021).
46. A. J. Andrews *et al.*, Ancient DNA SNP-panel data suggests stability in bluefin tuna genetic diversity despite centuries of fluctuating catches in the eastern Atlantic and Mediterranean. *Sci. Rep.* **11**, 20744 (2021).
47. L. Hauser, G. J. Adcock, P. J. Smith, J. H. B. Ramiréz, G. R. Carvalho, Loss of microsatellite diversity and low effective population size in an overexploited population of New Zealand snapper (Pagrus auratus). *Proc. Natl. Acad. Sci. U.S.A.* **99**, 11742–11747 (2002).
48. W. F. Hutchinson, C. van Oosterhout, S. I. Rogers, G. R. Carvalho, Temporal analysis of archived samples indicates marked genetic changes in declining North Sea cod (Gadus morhua). *Proc. Biol. Sci.* **270**, 2125–2132 (2003).
49. E. L. Cuveliers, F. A. M. Volckaert, A. D. Rijnsdorp, M. H. D. Larmuseau, G. E. Maes, Temporal genetic stability and high effective population size despite fisheries-induced life-history trait evolution in the North Sea sole. *Mol. Ecol.* **20**, 3555–3568 (2011).
50. G. Riccioni *et al.*, Spatio-temporal population structuring and genetic diversity retention in depleted Atlantic Bluefin tuna of the Mediterranean Sea. *Proc. Natl. Acad. Sci. U.S.A.* **107**, 2102–2107 (2010), 10.1073/pnas.0908281107.
51. B. S. Weir, C. C. Cockerham, Estimating f-statistics for the analysis of population structure. *Evolution* **38**, 1358–1370 (1984).
52. D. Shriner, G. Chen, A. Adeyemo, C. N. Rotimi, Estimation of F_{ST} and the Impact of de novo mutation. *Hum. Hered.* **82**, 37–49 (2016).
53. S. Kitada, R. Nakamichi, H. Kishino, Understanding population structure in an evolutionary context: Population-specific FST and pairwise FST. *G3* 11, jkab316 (2021).
54. J. R. Rooker *et al.*, Life history and stock structure of atlantic bluefin tuna (*Thunnus thynnus*). *Rev. Fish. Sci.* **15**, 265–310 (2007).
55. J. Carlsson *et al.*, Microsatellite and mitochondrial DNA analyses of Atlantic bluefin tuna (Thunnus thynnus thynnus) population structure in the Mediterranean Sea: Population genetics of mediterranean bluefin tuna. *Mol. Ecol.* **13**, 3345–3356 (2004).
56. A. M. Boustany, C. A. Reeb, B. A. Block, Mitochondrial DNA and electronic tracking reveal population structure of Atlantic bluefin tuna (Thunnus thynnus). *Mar. Biol.* **156**, 13–24 (2008).
57. J. Viñas *et al.*, Genetic population structure of European anchovy in the Mediterranean Sea and the Northeast Atlantic Ocean using sequence analysis of the mitochondrial DNA control region. *ICES J. Mar. Sci.* **71**, 391–397 (2013).
58. K. Čekovská *et al.*, Population genetic diversity of two marine gobies (Gobiiformes: Gobiidae) from the north-eastern atlantic and the mediterranean sea. *J. Mar. Sci. Eng.* **8**, 792 (2020).
59. R. Zardoya *et al.*, Differential population structuring of two closely related fish species, the mackerel (Scomber scombrus) and the chub mackerel (Scomber japonicus), in the Mediterranean Sea. *Mol. Ecol.* **13**, 1785–1798 (2004).
60. J. R. Alvarado Bremer, J. Viñas, J. Mejuto, B. Ely, C. Pla, Comparative phylogeography of Atlantic bluefin tuna and swordfish: The combined effects of vicariance, secondary contact, introgression, and population expansion on the regional phylogenies of two highly migratory pelagic fishes. *Mol. Phylogenet. Evol.* **36**, 169–187 (2005).
61. B. A. Block *et al.*, Electronic tagging and population structure of Atlantic bluefin tuna. *Nature* **434**, 1121–1127 (2005).
62. J.-M. Fromentin, D. Lopuszanski, Migration, residency, and homing of bluefin tuna in the western Mediterranean Sea. *ICES J. Mar. Sci.* **71**, 510–518 (2013).
63. K. Ferter *et al.*, Atlantic bluefin tuna tagged off Norway show extensive annual migrations, high site-fidelity and dynamic behaviour in the Atlantic Ocean and Mediterranean Sea. *Proc. Biol. Sci.* **291**, 20241501 (2024).
64. D. Brophy, N. Rodríguez-Ezpeleta, I. Fraile, H. Arrizabalaga, Combining genetic markers with stable isotopes in otoliths reveals complexity in the stock structure of Atlantic bluefin tuna (Thunnus thynnus). *Sci. Rep.* **10**, 14675 (2020).
65. K. Aarestrup *et al.*, First tagging data on large Atlantic bluefin tuna returning to Nordic waters suggest repeated behaviour and skipped spawning. *Sci. Rep.* **12**, 11772 (2022).
66. B. R. MacKenzie, P. Mariani, Spawning of bluefin tuna in the Black Sea: Historical evidence, environmental constraints and population plasticity. *PLoS ONE* **7**, e39998 (2012).
67. A. Di Natale, Review of the historical and biological evidences about a population of bluefin tuna (*Thunnus thynnus* L.) in the eastern Mediterranean and the Black Sea. *Col Vol. Sci. Pap. ICCAT* **71**, 1098–1124 (2015).
68. G. De Luca, P. Mariani, B. R. MacKenzie, M. Marsili, Fishing out collective memory of migratory schools. *J. R. Soc. Interface* **11**, 20140043 (2014).
69. M. Sodeland *et al.*, Stabilizing selection on Atlantic cod supergenes through a millennium of extensive exploitation. *Proc. Natl. Acad. Sci. U.S.A.* **119**, e2114904119 (2022).
70. R. S. Waples, Separating the wheat from the chaff: Patterns of genetic differentiation in high gene flow species. *J. Hered.* **89**, 438–450 (1998).
71. R. S. Waples, What is Ne, anyway? *J. Hered.* **113**, 371–379 (2022), 10.1093/jhered/esac023.
72. A. Di Natale, M. Idrissi, Factors to be taken into account for a correct reading of tuna trap catch series. *Collect. Vol. Sci. Pap. ICCAT/Recl. Doc. Sci. CICTA/Colecc. Doc. Cient. CICAA* **67**, 242–261 (2012).
73. L. M. Atmore *et al.*, The once and future fish: 1300 years of Atlantic herring population structure and demography revealed through ancient DNA and mixed-stock analysis. bioRxiv [Preprint] (2024). https://doi.org/10.1101/2024.07.11.603078 (Accessed 16 June 2024).
74. T. Oosting *et al.*, Mitochondrial genomes reveal mid-Pleistocene population divergence, and post-glacial expansion, in Australasian snapper (*Chrysophrys auratus*). *Heredity* **130**, 1–10 (2022), 10.1038/s41437-022-00579-1.
75. L. Martínez-García *et al.*, Historical demographic processes dominate genetic variation in Ancient Atlantic cod mitogenomes. *Front. Ecol. Evol.* **9**, 342 (2021).
76. C. F. Speller *et al.*, High potential for using DNA from ancient herring bones to inform modern fisheries management and conservation. *PLoS ONE* **7**, e51122 (2012).
77. S. Bonanomi *et al.*, Archived DNA reveals fisheries and climate induced collapse of a major fishery. *Sci. Rep.* **5**, 15395 (2015).
78. E. E. Nielsen, M. M. Hansen, V. Loeschcke, Analysis of microsatellite DNA from old scale samples of Atlantic salmon Salmo salar: A comparison of genetic composition over 60 years. *Mol. Ecol.* **6**, 487–492 (1997).
79. F. J. Mather, J. M. Mason, A. C. Jones, Historical document: Life history and fisheries of Atlantic bluefin tuna. *NOAA technical memorandum NMFS-SEFSC* **370**, 1–165 (1995).
80. R. Frankham, Genetics and extinction. *Biol. Conserv.* **126**, 131–140 (2005).
81. R. S. Waples, P. M. Grewe, M. W. Bravington, R. Hillary, P. Feutry, Robust estimates of a high Ne/N ratio in a top marine predator, southern bluefin tuna. *Sci. Adv.* **4**, eaar7759 (2018).
82. G. N. Puncher *et al.*, Individual assignment of Atlantic bluefin tuna in the northwestern Atlantic Ocean using single nucleotide polymorphisms reveals an increasing proportion of migrants from the eastern Atlantic Ocean. *Can. J. Fish. Aquat. Sci.* **79**, 111–123 (2022).
83. S. Gopalakrishnan *et al.*, The population genomic legacy of the second plague pandemic. *Curr. Biol.* **32**, 4743–4751.e6 (2022).
84. M. Kardos, R. S. Waples, Low-coverage sequencing and Wahlund effect severely bias estimates of inbreeding, heterozygosity and effective population size in North American wolves. *Mol. Ecol.* **24**, e17415 (2024).
85. D. Hedgecock, No evidence for temporally balanced selection on larval Pacific oysters Crassostrea gigas: A comment on Durland et al. (2021). *Proc. Biol. Sci.* **289**, 20212579 (2022).
86. J. A. Coombs, B. H. Letcher, K. H. Nislow, GONe: Software for estimating effective population size in species with generational overlap. *Mol. Ecol. Resour.* **12**, 160–163 (2012).
87. I. Novo *et al.*, Impact of population structure in the estimation of recent historical effective population size by the software GONE. *Genet. Sel. Evol.* **55**, 86 (2023).
88. N. Barghi, J. Hermisson, C. Schlötterer, Polygenic adaptation: A unifying framework to understand positive selection. *Nat. Rev. Genet.* **21**, 769–781 (2020).
89. M. Dehasque *et al.*, Inference of natural selection from ancient DNA. *Evol. Lett.* **4**, 94–108 (2020).
90. M. Kimura, Attainment of quasi linkage equilibrium when gene frequencies are changing by natural selection. *Genetics* **52**, 875–890 (1965).
91. S. Yeaman, Evolution of polygenic traits under global vs local adaptation. *Genetics* **220**, iyab134 (2022).
92. E. F. Eriksen *et al.*, Five millennia of mitonuclear discordance in Atlantic bluefin tuna identified using ancient DNA. *Heredity* **134**, 175–185 (2025).
93. B. Llamas *et al.*, From the field to the laboratory: Controlling DNA contamination in human ancient DNA research in the high-throughput sequencing era. *STAR: Sci. Technol. Archaeol. Res.* **3**, 1–14 (2017).
94. C. Renfrew, K. Boyle, *Archaeogenetics: DNA and thE Population Prehistory of Europe* (Academic Press, 2024).
95. J. Dabney *et al.*, Complete mitochondrial genome sequence of a Middle Pleistocene cave bear reconstructed from ultrashort DNA fragments. *Proc. Natl. Acad. Sci. U.S.A.* **110**, 15758–15763 (2013).
96. P. Serventi *et al.*, Iron Age Italic population genetics: The Piceni from Novilara (8th–7th century BC). *Ann. Hum. Biol.* **45**, 34–43 (2018).
97. P. B. Damgaard *et al.*, Improving access to endogenous DNA in ancient bones and teeth. *Sci. Rep.* **5**, 11184 (2015).
98. V. P. Cruz *et al.*, Identification and validation of single nucleotide polymorphisms as tools to detect hybridization and population structure in freshwater stingrays. *Mol. Ecol. Resour.* **17**, 550–556 (2017).
99. A. Blanquer, "Phylogéographie intraspécifique d'un poisson marin, le flet Platichthys flesus L. (Heterosomata): Polymorphisme des marqueurs nucléaires et mitochondriaux," PhD thesis (Université des Sciences et Techniques du Languedoc, Montpellier, France, 1990).
100. J. D. Kapp, R. E. Green, B. Shapiro, A Fast and Efficient single-stranded genomic library preparation method optimized for ancient DNA. *J. Hered.* **112**, 241–249 (2021).
101. Next-Generation BFT Consortium, *Short-Term Contract for Biological Studies (iccat Gbyp 08/2017-2) of The Atlantic-wide Research Programme on Bluefin Tuna (GBYP phase 7).* https://www.iccat.int/GBYP/Docs/Biological_Studies_Phase_7_NextGeneration_BFT.pdf. Accessed 1 October 2024.
102. B. Bushnell *"BBMap: A Fast, Accurate, Splice-aware Aligner" Lawrence Berkeley National Lab* (LBNL, Berkeley, CA, 2014).
103. A. M. Bolger, M. Lohse, B. Usadel, Trimmomatic: A flexible trimmer for Illumina sequence data. *Bioinformatics* **30**, 2114–2120 (2014).
104. M. Schubert *et al.*, Characterization of ancient and modern genomes by SNP detection and phylogenomic and metagenomic analysis using PALEOMIX. *Nat. Protoc.* **9**, 1056–1082 (2014).
105. M. Schubert, S. Lindgreen, L. Orlando, AdapterRemoval v2: Rapid adapter trimming, identification, and read merging. *BMC Res. Notes* **9**, 88 (2016).

106. H. Jónsson, A. Ginolhac, M. Schubert, P. L. F. Johnson, L. Orlando, mapDamage2.0: Fast approximate Bayesian estimates of ancient DNA damage parameters. *Bioinformatics* **29**, 1682–1684 (2013).
107. A. McKenna *et al.*, The genome analysis toolkit: A mapreduce framework for analyzing next-generation DNA sequencing data. *Genome Res.* **20**, 1297–1303 (2010).
108. G. Jun, M. K. Wing, G. R. Abecasis, H. M. Kang, An efficient and scalable analysis framework for variant extraction and refinement from population-scale DNA sequence data. *Genome Res.* **25**, 918–925 (2015).
109. H. Li *et al.*, The sequence alignment/map format and SAMtools. *Bioinformatics* **25**, 2078–2079 (2009).
110. P. Danecek *et al.*, The variant call format and VCFtools. *Bioinformatics* **27**, 2156–2158 (2011).
111. S. Picq, W. O. McMillan, O. Puebla, Population genomics of local adaptation versus speciation in coral reef fishes (Hypoplectrus spp, Serranidae). *Ecol. Evol.* **6**, 2109–2124 (2016).
112. S. J. Amish *et al.*, Assessing thermal adaptation using family-based association and FST outlier tests in a threatened trout species. *Mol. Ecol.* **28**, 2573–2593 (2019).
113. F. Pappas *et al.*, Whole-genome re-sequencing provides key genomic insights in farmed Arctic charr (Salvelinus alpinus) populations of anadromous and landlocked origin from Scandinavia. *Evol. Appl.* **16**, 797–813 (2023).
114. J. Yuan *et al.*, How genomic insights into the evolutionary history of clouded leopards inform their conservation. *Sci. Adv.* **9**, eadh9143 (2023).
115. S. Purcell *et al.*, PLINK: A tool set for whole-genome association and population-based linkage analyses. *Am. J. Hum. Genet.* **81**, 559–575 (2007).
116. A. Abdellaoui *et al.*, Population structure, migration, and diversifying selection in the Netherlands. *Eur. J. Hum. Genet.* **21**, 1277–1285 (2013).
117. N. Patterson *et al.*, *EIGENSOFT version 5.01* (Harvard University, 2013).
118. E. Elhaik, Principal Component Analyses (PCA)-based findings in population genetic studies are highly biased and must be reevaluated. *Sci. Rep.* **12**, 14683 (2022).
119. J. K. Pritchard, M. Stephens, P. Donnelly, Inference of population structure using multilocus genotype data. *Genetics* **155**, 945–959 (2000).
120. G. Evanno, S. Regnaut, J. Goudet, Detecting the number of clusters of individuals using the software STRUCTURE: A simulation study. *Mol. Ecol.* **14**, 2611–2620 (2005).
121. D. A. Earl, B. M. vonHoldt, Structure harvester: A website and program for visualizing STRUCTURE output and implementing the Evanno method. *Conserv. Genet. Re.* **4**, 2 (2012), 10.1007/s12686-011-9548-7.
122. N. M. Kopelman, J. Mayzel, M. Jakobsson, N. A. Rosenberg, I. Mayrose, Clumpak: A program for identifying clustering modes and packaging population structure inferences across K. *Mol. Ecol. Resour.* **15**, 1179–1191 (2015).
123. M. Nei, *Molecular Evolutionary Genetics* (Columbia University Press, 1987), pp. 433–496. http://dx.doi.org/10.7312/nei-92038.
124. R. Meyermans, W. Gorssen, N. Buys, S. Janssens, How to study runs of homozygosity using PLINK? A guide for analyzing medium density SNP data in livestock and pet species *BMC Genomics* **21**, 94 (2020).
125. E. Santiago *et al.*, Recent demographic history inferred by high-resolution analysis of linkage disequilibrium. *Mol. Biol. Evol.* **37**, 3642–3653 (2020).
126. K. Luu, E. Bazin, M. G. B. Blum, pcadapt: An R package to perform genome scans for selection based on principal component analysis. *Mol. Ecol. Resour.* **17**, 67–77 (2017).
127. M. C. Whitlock, K. E. Lotterhos, Reliable detection of loci responsible for local adaptation: Inference of a null model through trimming the distribution of FST. *Am. Nat.* **186**, S24–S36 (2015).
128. A. Cariani, Ancient DNA suggests a historical demographic decline and genetic erosion in the Atlantic bluefin tuna. BioProject NCBI. https://www.ncbi.nlm.nih.gov/sra/PRJNA1238330. Deposited 14 May 2025.
129. A. Cariani, An improved draft genome assembly and annotation for the iconic Atlantic bluefin tuna (Thunnus thynnus). BioProject NCBI. https://www.ncbi.nlm.nih.gov/bioproject/PRJNA408269. Deposited 16 February 2022.